ORIGINAL PAPER

Seismic microzonation of Ubhur district, Jeddah, Saudi Arabia, using H/V spectral ratio

Maher Aldahri[1] · Mahmoud El-Hadidy[2] · Hani Zahran[1] · Kamal Abdelrahman Hassanein[2,3]

Abstract

Ubhur district is the northern extension of Jeddah. A lot of the new investments and mega structures will be constructed in this area; the highest skyscraper in the Arabian Gulf region will be built in Ubhur. The surface geology of the investigated region is complex, where the sabkha deposits spread everywhere. The subsurface structure of the subsurface soil is complex and includes different soil classes. Microtremor data was acquired at 76 sites located in Ubhur district. The horizontal to vertical spectral ratio technique is used to determine the resonance frequency (f_0) and the maximum amplification factor (A_0) at the selected sites. This technique is considered as the cheapest and most reliable one for determining the resonance frequency. The acquired data was processed using the Geopsy software where the reliability of the H/V curves and peaks was considered through the data processing and analysis. The results indicate that the predominant resonance frequency of Ubhur district ranges between 0.77 and 5.7 Hz, while the maximum amplification factors range from 2 to 6. It is indicated that the central zone of the Ubhur district is considered suitable for the construction of high-rise facilities compared to other parts of the region, which should be taken into consideration during land use planning.

Keywords Amplification factor · Resonance frequency · Land use planning · Ubhur · Saudi Arabia

Introduction

Ubhur district is located at the eastern coast of the Red Sea to the north of Jeddah city. It is considered as the northern extension of Jeddah city, where most of the new investments and constructions are located. It extends from the north of King Abdul-Aziz International Airport in the south to Asfan Road in the north. Figure 1 shows the location of the study area and its surface geology.

The Arabian Plate is a single tectonic plate, which is surrounded by relatively high active tectonic zones (Fig. 2). Active tectonics of the region is dominated by the collision of the Arabian Plate with the Eurasian Plate along the Zagros and Bitlis thrust systems, rifting and seafloor spreading in the Red Sea and Gulf of Aden, and strike-slip faulting occurs along the Gulf of Aqaba Dead Sea fault system. It is evident that the strong earthquakes, as well as most of the microearthquakes, have occurred at previously defined active tectonic trends (Fig. 2). The Gulf of Aqaba is the source of the 22 November 1995 earthquake (Ms = 7.3), which is the largest recent earthquake which shocked the Kingdom (Roobol et al. 1999). Since 1900, some moderate and large intraplate earthquakes hit the Arabian Peninsula; for example, Ambraseys et al. (1994) mentioned the Sa'dah earthquake on 11 January 1941 with Ms = 6.5. Recently, the Saudi National Seismological Network detected several moderate earthquakes within the Arabian Shield; El-hadidy (2015) also mentioned these earthquakes (e.g., Tabuk earthquake on 22 June 2004 (Mw = 5.1), Harrat Lunayyir earthquake on 19 May 2009 (Mw = 5.7), and Sabia earthquake on 21 January 2015 (M_L = 5.1)). Figure 3 shows the seismicity of the Arabian Peninsula and its surroundings (Zahran et al. 2016).

Al-Qarni (2015) studied the microzonation of the urban area of Jeddah starting from the Jeddah Islamic Port in the south to the King Abdul-Aziz International Airport in the

✉ Kamal Abdelrahman Hassanein
khassanein@ksu.edu.sa

[1] Saudi Geological Survey, Jeddah, Saudi Arabia

[2] Seismology Department, National Research Institute of Astronomy and Geophysics, Cairo, Egypt

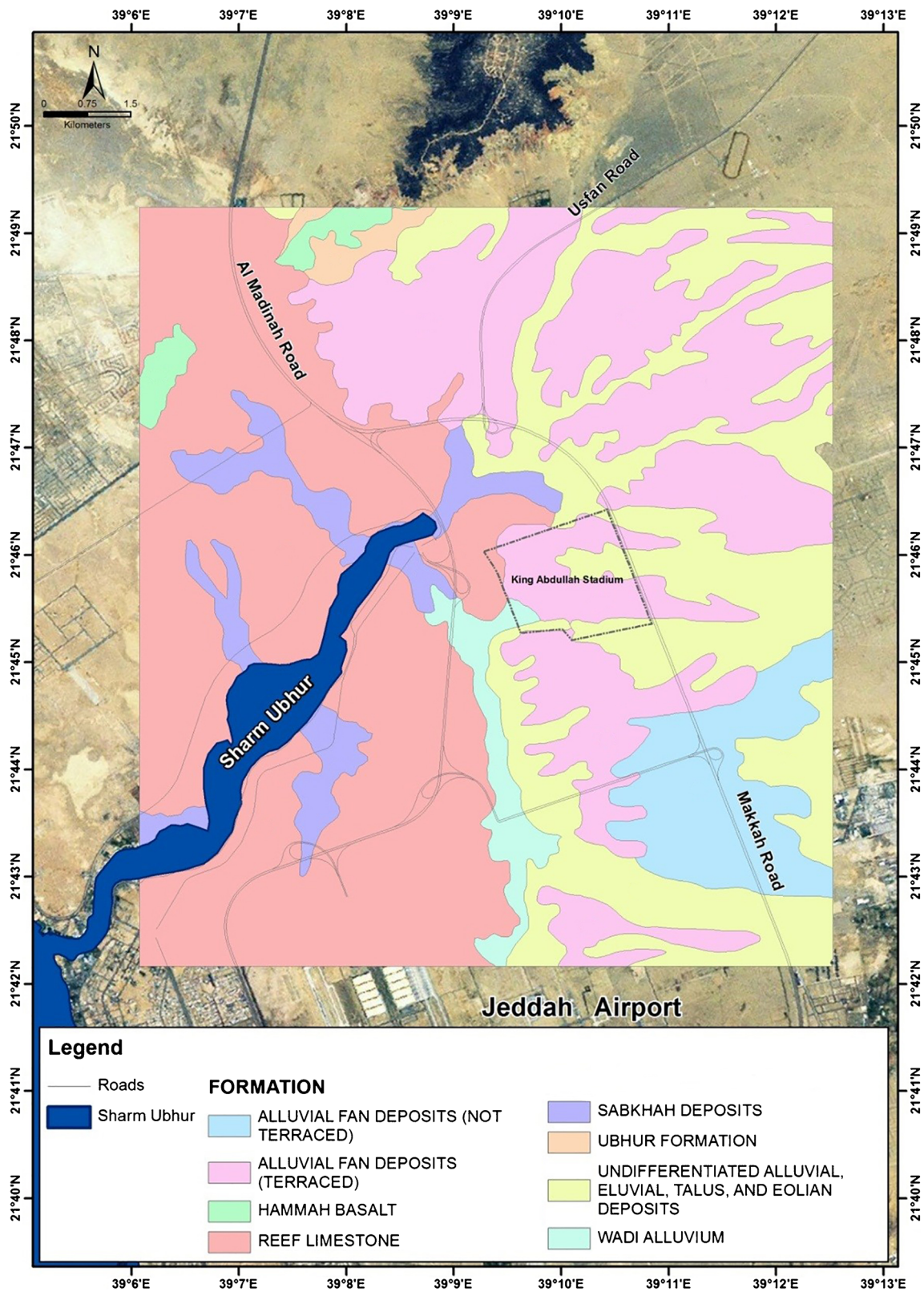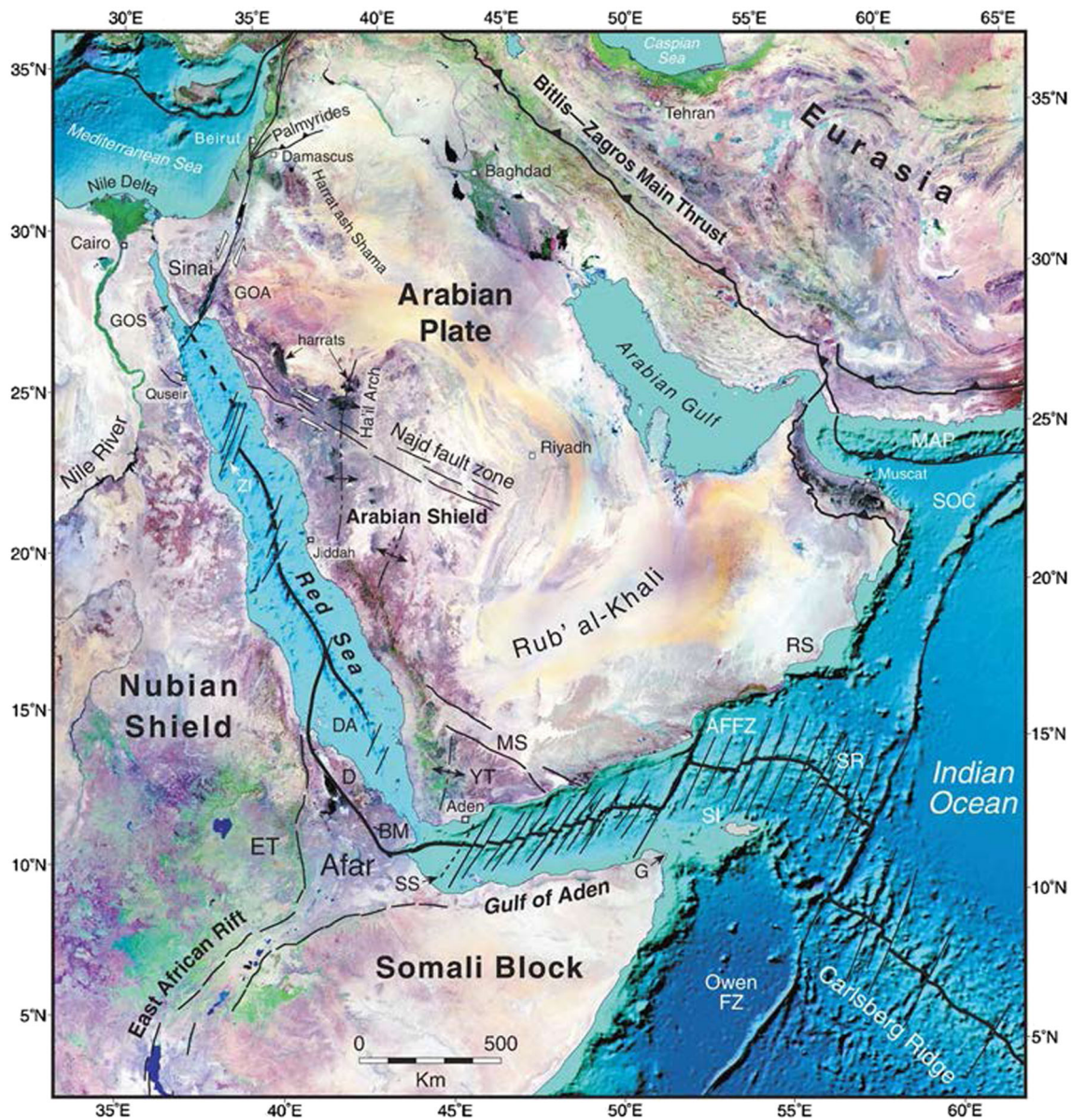[3] Geology and Geophysics Department, King Saud University, Riyadh, Saudi Arabia

Fig. 1 Location and geologic map of Ubhur area (after Johnson 1999)

north. Al-Qarni (2015) acquired microtremor data at 155 sites and 57 (1D) profiles of the multichannel analysis of surface waves (MASW). The results of the microtremor analysis show that f_0 ranges between 0.48 and 4.87 Hz.

Fig. 2 Major tectonic elements surrounding Saudi Arabia. The Pan-African Najd fault system, the Aqaba–Levant intracontinental transform boundary, the Mediterranean–Bitlis–Zagros convergence zone, and the East African rift are highlighted. AFFZ = Alula-Fartak fracture zone; BM = Bab al Mandeb; D = Danakil horst; DA = Dahlak Archipelago; ET = Ethiopian trap series; G = Cape Guardafui; GOA = Gulf of Aqaba; GOS = Gulf of Suez; MAP = Makran accretionary prism; MER = main Ethiopian rift; MS = Mesozoic Marib-Shabwa (Sab'atayn) Basin; SI = Socotra Island; SOC = Semail oceanic crust; SR = Sheba Ridge; SS = Shukra al Sheik discontinuity; RS = Ras Sharbithat; YT = Yemen trap series; ZI = Zabargad Island (After Bosworth et al. 2005)

This wide range of f_0 reflects the complex and variant structure of the surface of soil in Jeddah. According to Vs_{30} measurements, the study area was divided into site classes D, C, and B.

The occurrence of such moderate earthquakes close to the urban areas built on weak soils can cause significant damage; therefore, the use of the produced f_0 and A_0 distribution maps is very important for seismic risk reduction in the Ubhur district.

Geological setting of northern Jeddah

According to the studies of Morris (1975), Bahafzullah et al. (1993), Al-Saifi and Qari (1996), and Aqeel (2007), the geological setting of northern Jeddah (including Ubhur district) can be classified into (1) hills of Precambrian igneous and metamorphic rocks, (2) alluvial fan deposits and sand bodies, (3) isolated lagoons and sabkha deposits, and 4) near-shore marine deposits and
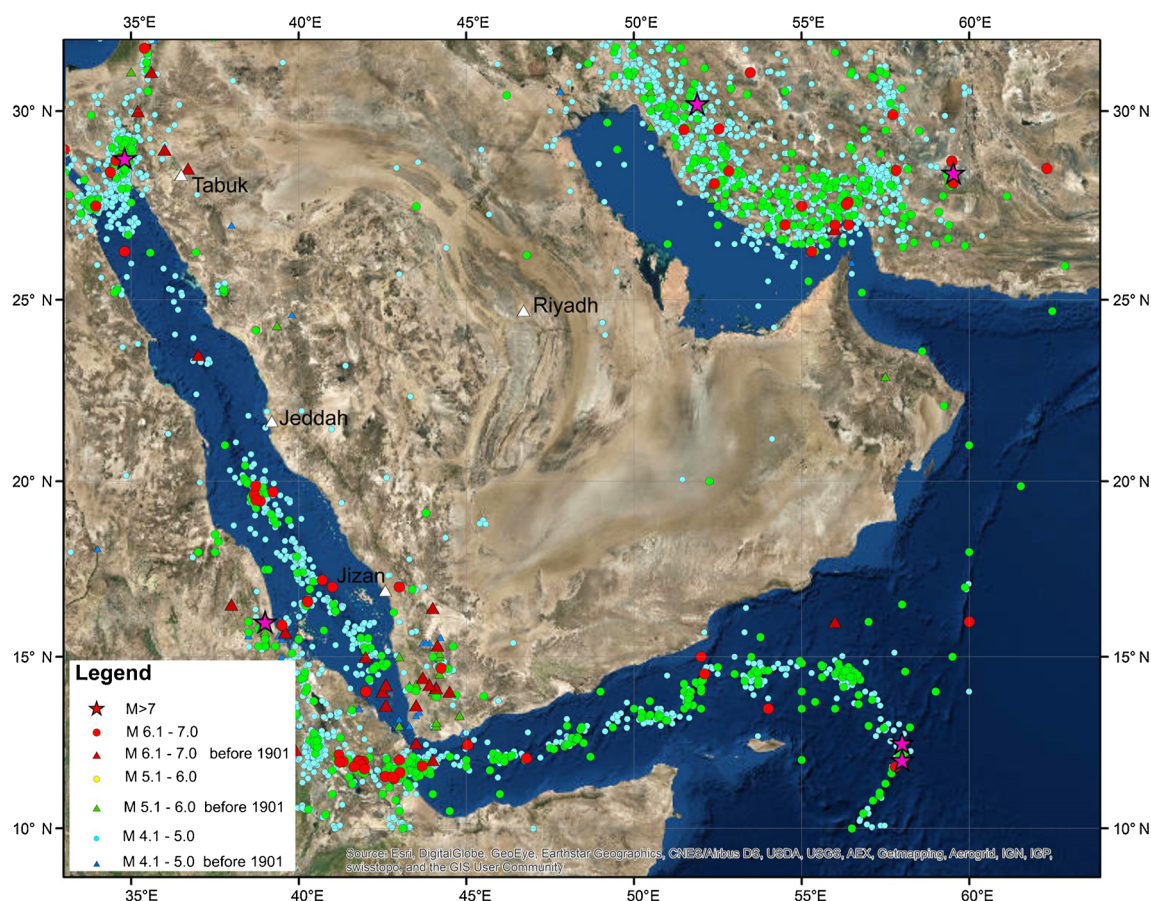
Fig. 3 Distribution of epicenters of shallow earthquakes (depth < 30 km) and M > 4 in and around the Arabian Peninsula which occurred up to May 2015 (Zahran et al. 2016)

coralline terrace. The Saudi Geological Survey (SGS) produced a surface geology map of the study area, as a part of a large-scale geology map of the western Saudi Arabia. Figure 1 shows the geologic setting of the Ubhur area (Johnson 1999).

Bahafzullah et al. (1993) studied the geological setting of northern Jeddah and identified three distinct geomorphological assemblages. The first assemblage starts from the west and includes near-shore marine deposits and is composed of a coralline terrace, which extends a few meters above the mean sea level. The second assemblage consists of isolated lagoonal sediments and salt-encrusted intertidal flats. The third assemblage lies to the east and is occupied by a veneer of alluvial fans, eolian sand bodies, and wadi plains. In addition, other features include isolated remnants and dissected hills of Precambrian crystalline rocks and outcrops of tilted and faulted Tertiary clastic sedimentary rocks. In some areas, the Tertiary deposits and the Precambrian rocks are capped by flat-lying basalt of Harrat Rahat and its erosional remnants.

Geotechnical and Vs_{30} data

Ali and Hossain (1988) studied the geotechnical and geochemical characteristics of Ubhur subsoils. They investigated the soil up to 15-m depth and classified the soil composition of northern Jeddah into five soil units and three rock units. The classified units are illustrated in Fig. 4, and they are (1) gray to light brown soft to medium sensitive sandy silty clay with gypsum crystals and shells, (2) stiff to very stiff brown sandy silty clay, (3) gray very loose to loose silty sand and sandy silt, (4) light brown to gray very loose carbonate silty sand, (5) gray medium carbonate gravelly sand, (6) yellowish to creamy white coarse-grained shelly coralline limestone, weak to moderately weak, (7) Tertiary to Quaternary basalt, and (8) tertiary deposits of sandstone, siltstone, or claystone.

Ali and Hossain have also divided the study area into seven zones as the following:

Zone I occupies the northern area of the Ubhur district and consists of soft clay (unit 1) overlying stiff clay (unit 2) underlain either by medium dense carbonate gravelly sand (unit
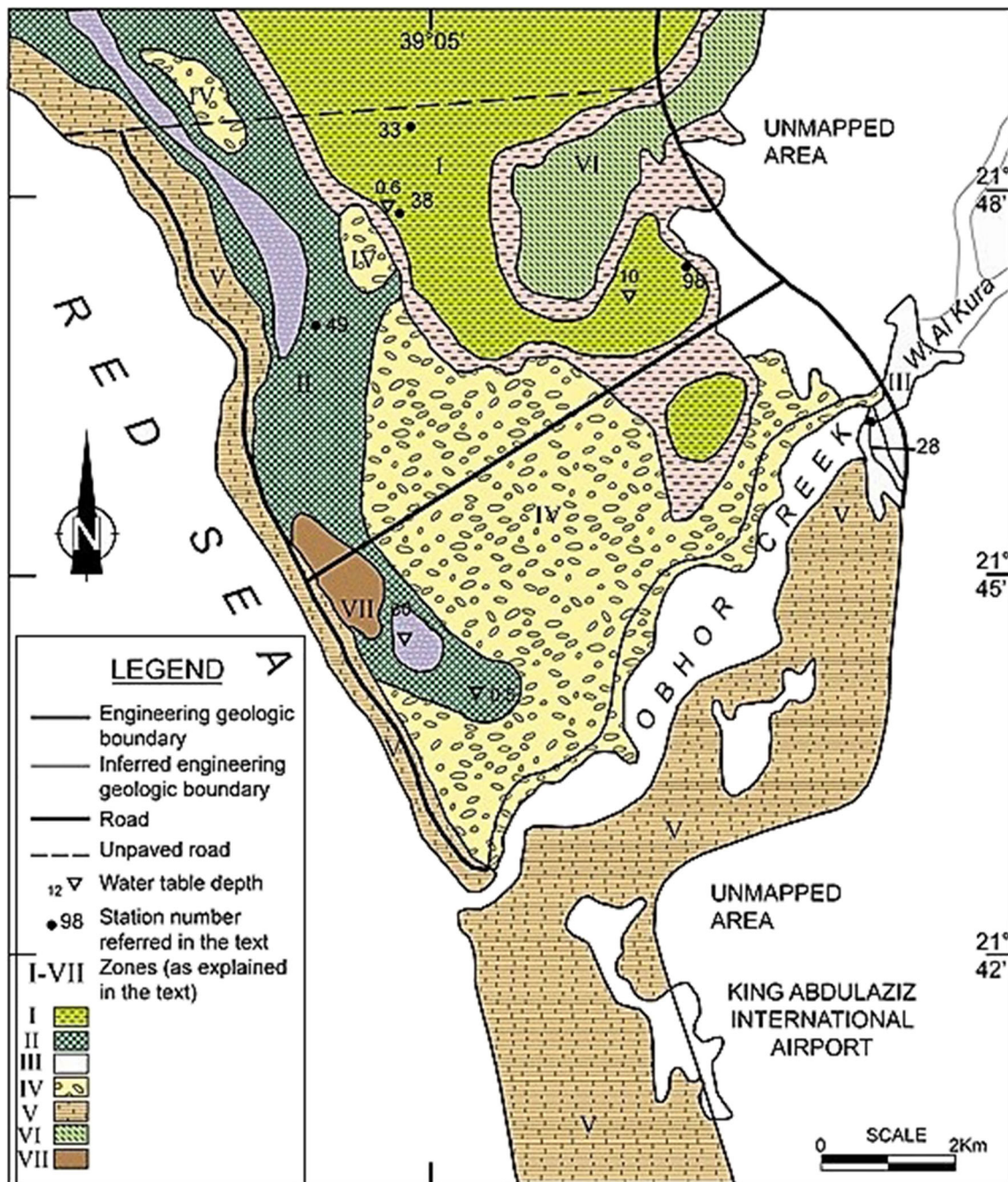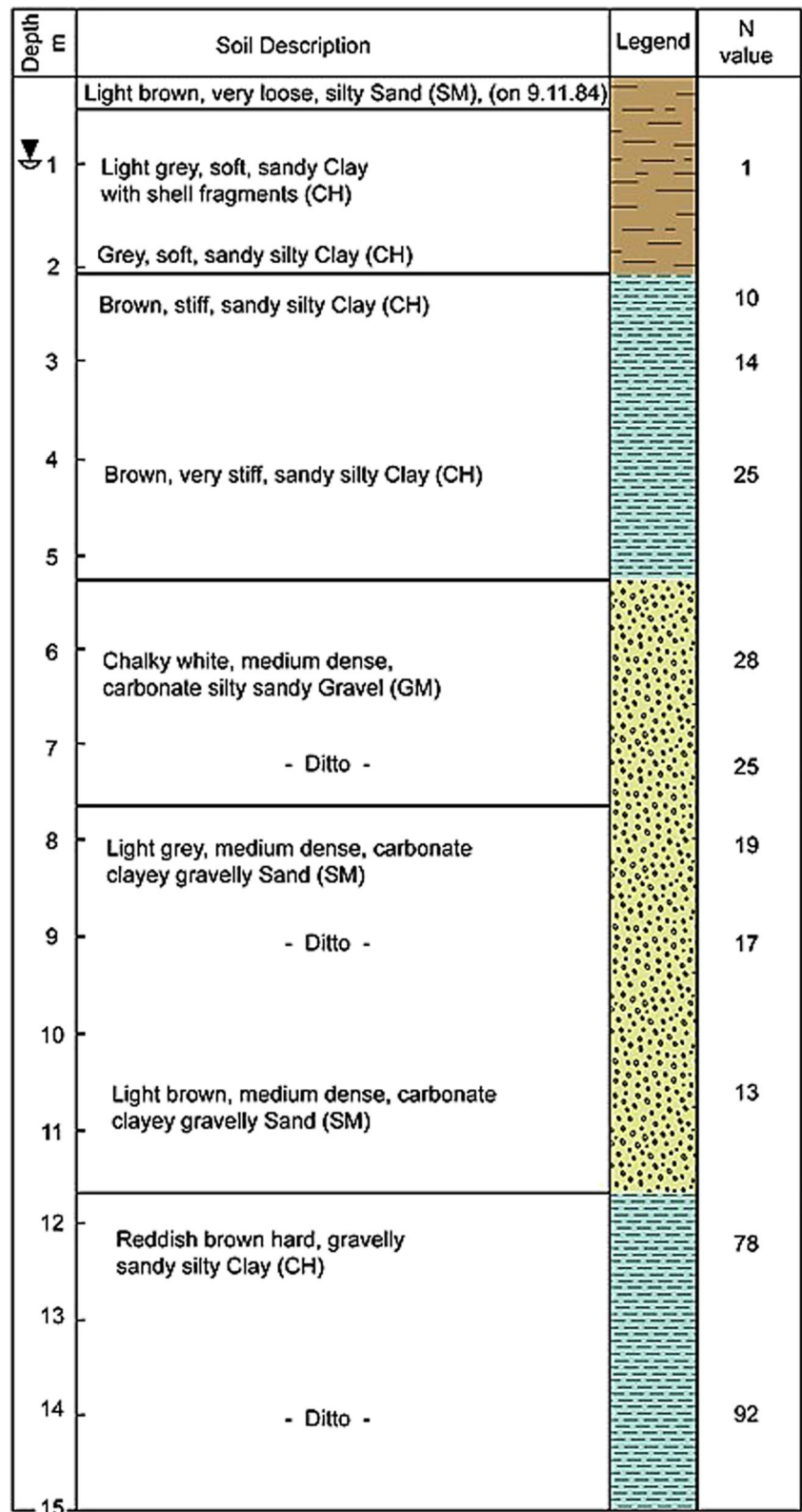
Fig. 4 The identified rock and soil units in Ubhur area (After Ali and Hossain 1988)

5) or by a hard clay or claystone (unit 8). The soil profile of zone I is described in Fig. 5.

Zone II extends parallel to the coast in the north Ubhur district and is composed of loose carbonate silty sand (unit 4) which occurs as gravelly sand (unit 5, whose lowest 1 m is very dense), underlain by coralline limestone (unit 6). The soil column of this soil is shown in Fig. 6.

Zone III covers a small area about 1 km² at the up-stream end of Ubhur creek. Unit 3 is constituted by very loose silty sand with about 11-m thickness whose lower part is slightly clayey overlying a layer of soft clay (unit 1) which is underlain by medium dense carbonate gravelly sand. Figure 7 presents the soil profile of this zone. This zone is considered as part of Wadi Al-Kura which

Fig. 5 Zone I soil profile (After
Ali and Hossain 1988)

Depth m	Soil Description	Legend	N value
	Light brown, very loose, silty Sand (SM), (on 9.11.84)		
1	Light grey, soft, sandy Clay with shell fragments (CH)		1
2	Grey, soft, sandy silty Clay (CH)		
	Brown, stiff, sandy silty Clay (CH)		10
3			14
4	Brown, very stiff, sandy silty Clay (CH)		25
5			
6	Chalky white, medium dense, carbonate silty sandy Gravel (GM)		28
7	- Ditto -		25
8	Light grey, medium dense, carbonate clayey gravelly Sand (SM)		19
9	- Ditto -		17
10			
11	Light brown, medium dense, carbonate clayey gravelly Sand (SM)		13
12	Reddish brown hard, gravelly sandy silty Clay (CH)		78
13			
14	- Ditto -		92
15			

originates from the crystalline rocks eastward and was
linked to the creek.

Zone IV includes a major terrace and two minor ones of
medium dense carbonate gravelly sand (unit 5) covering an

Fig. 6 Zone II soil profile (After Ali and Hossain 1988)

Depth m	Material Description	Legend	N value
	Brown cemented sandy crust (SM)		
1	Chalky white, very loose, carbonate silty Sand with shell fragments (SM) (on 10.11.84)		3
2	Light grey, loose, carbonate gravelly silty Sand (SM)		8
3	Bluish grey, medium dense, carbonate silty gravelly Sand (SM)		22
4	Light grey, medium dense, carbonate silty gravelly Sand (SM)		23
5	- Ditto, but dense		31
6	Dark grey, very dense, carbonate silty sandy Gravel (GM)		80
7			
8	Yellowish to creamy white, coarse grained shelly Coralline Limestone, moderately weak		
9	End of Boring		

area about 22 km^2 at the northern bank of Ubhur creek. A thin layer of about 10 cm thick consisting mostly of aeolian sand covers this area.

Zone V is located at the south of the Ubhur creek as well as a belt about 0.5 km wide along the coast in northern Ubhur; in the southern part, the limestone is sometimes covered by a thin layer of carbonate gravelly sand, the larger thickness being in the areas away from the coast. Morris (1975) illustrated the occurrence of compact limestone which has an N value of 50

beneath the King Abdulaziz International Airport. This limestone has a thickness range between 2.5 and 10 m.

Zone VI contains a hill of gravelly sand or sandy gravel layers underlain by layers of red or chalky hard clays or mudstone or friable sandstone (unit 8) and capped with basaltic lava (unit 7).

Zone VII covers a small area within zone II as a layer of soft clay about 2.5 m thick similar to the soft clay of zone I, overlying medium dense carbonate gravelly sand. At one location in this zone, large gypsum crystals (probably part of a

Fig. 7 Zone III soil profile (After Ali and Hossain 1988)

gypsum layer) were found at depths of 0.5 to 0.6 m, and this layer affected the geotechnical parameters.

Aldahri et al. (2017) measured the Vs$_{30}$ at 76 sites within the study area using the multiple analysis of surface wave
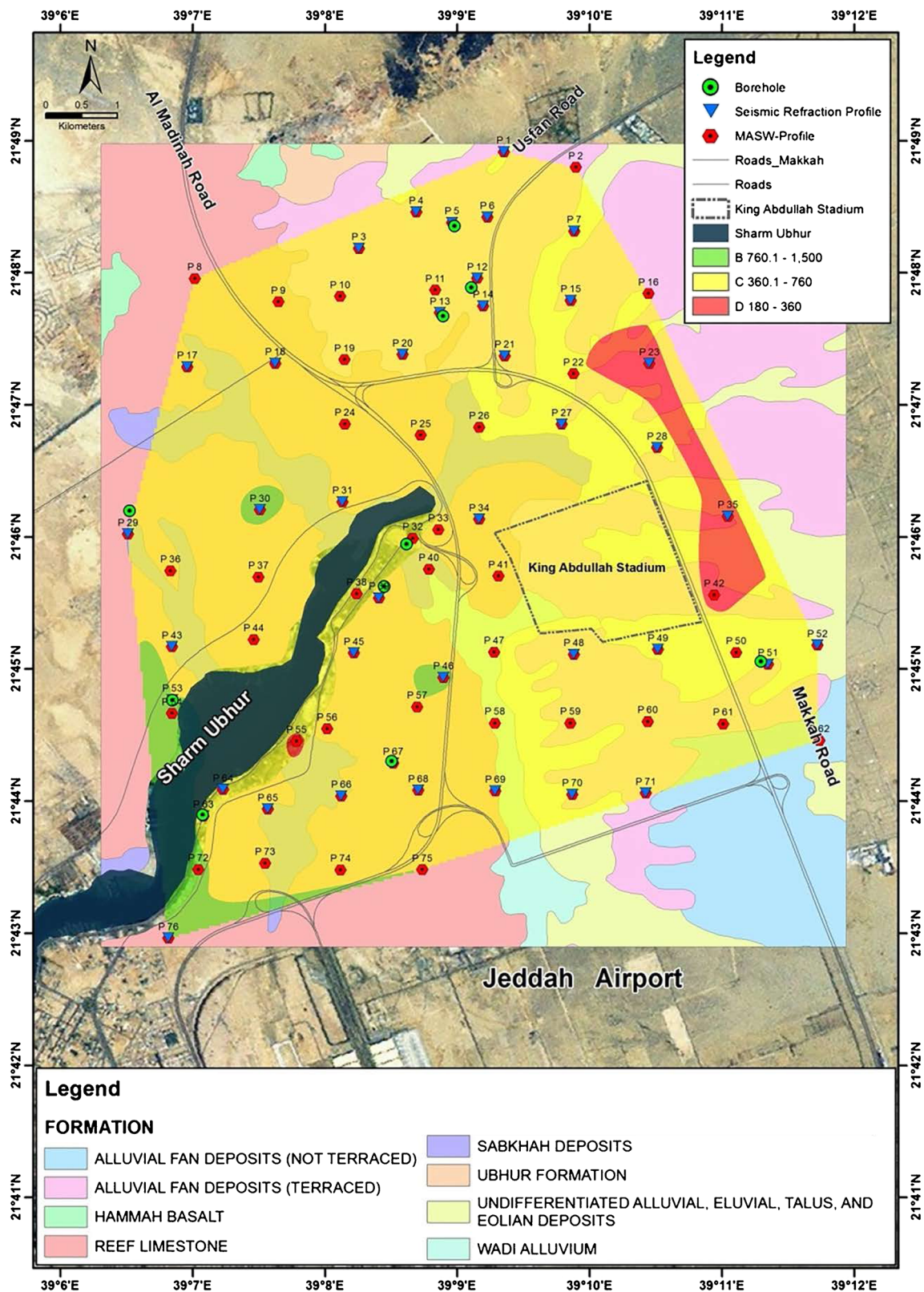
Fig. 8 Map showing the soil classes and distribution of boreholes in the study area (Aldahri et al. 2017)

(MASW) technique and the N value obtained from 10 boreholes having a depth range of 10 to 15 m (Fig. 8). They classified the Ubhur district into three soil classes based on the NEHRB classification of B, C, and D as shown in Fig. 8.
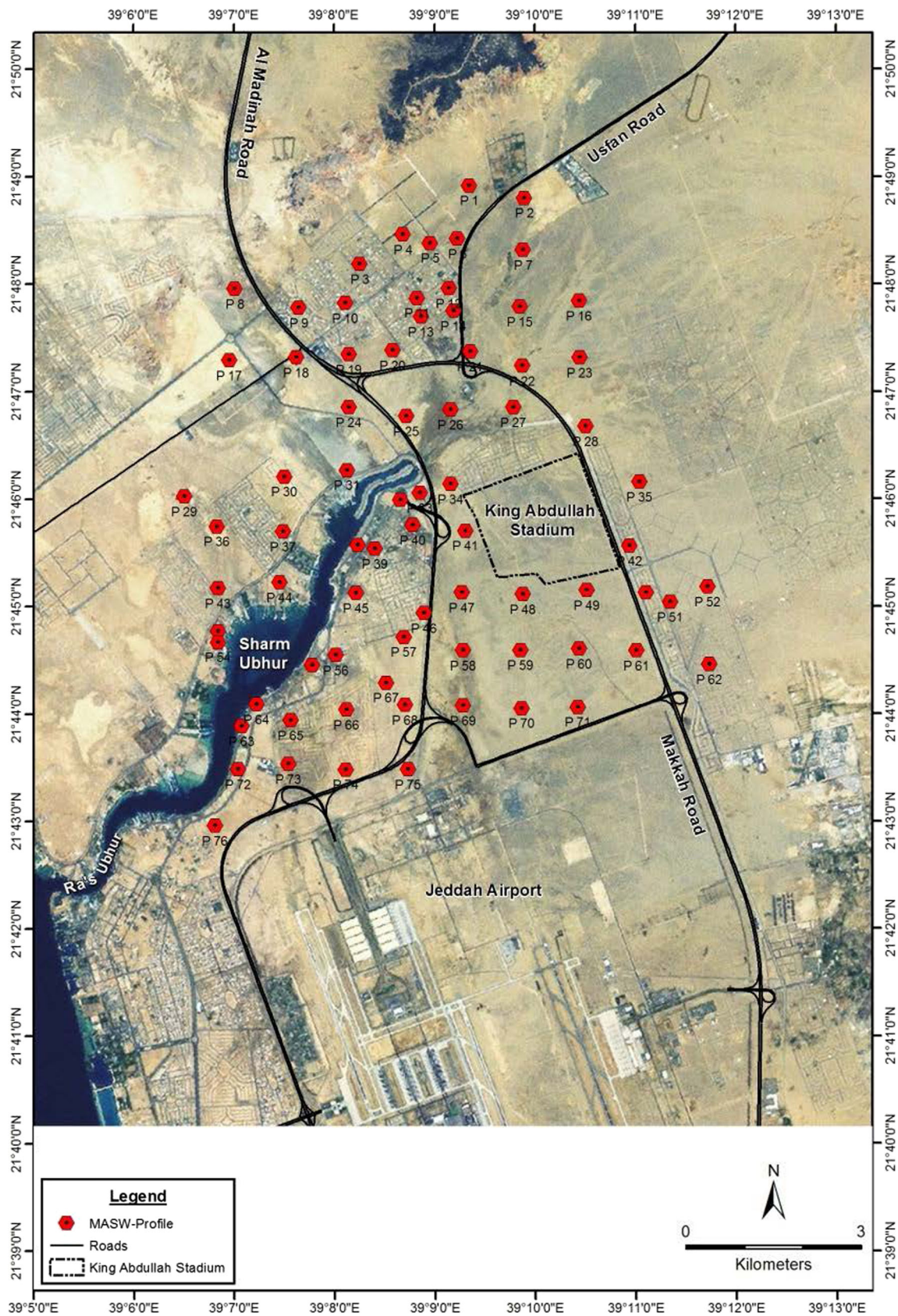
Fig. 9 Selected sites for microtremor data acquisition

Site class B occupies a thin strip at the western part of the Ubhur district, while site class C occupies the central part of the study area. It occupies more than 90% of the surface area of Ubhur.

Methodology of the H/V spectral ratio

Nakamura (1989) proposed the basis of qualitative arguments that the H/V ratio is a reliable technique of the site response to S-wave, providing reliable estimates, not only of the resonance frequency, but also of the corresponding amplification. These ratios are much more stable than the noise spectra and that, on soft soil sites, they display a clear peak that is well correlated with the fundamental resonance frequency.

The basic concept of Nakamura's technique is described as follows. The transfer function (site effect) ST of the surface layers is generally defined as

$$ST = SHs/SHB \qquad (1)$$

where SHs is the horizontal tremor spectrum on the surface, and SHB is the horizontal tremor spectrum incident from the substrate (rock or firm soil) to the surface layers. But the SHs of microtremors is readily affected by the surface waves. The effect of Rayleigh waves should be included in the vertical tremor spectrum SVs on the surface, but not included in the vertical tremor spectrum SVB in the base ground (rock). The effect of Rayleigh waves on the vertical tremor is

$$ES = SVs/SVB \qquad (2)$$

If there is no Rayleigh waves, ES = 1, ES will take a value larger than 1 with increasing effect of the Rayleigh wave. The value of ST/ES may be considered to offer a more reliable transfer function STT after elimination of the effect of Rayleigh waves (Nakamura 1989; Lermo and Chaves-Garcia 1993).

$$STT = ST/ES = RS/RB \qquad (3)$$

where RS = SHs / SVS and RB = SHB / SVB.

RS and RB were obtained by dividing the horizontal tremor spectrum by the vertical spectrum, corresponding to surface and bedrock tremors, respectively. In the firm substrate, propagation is even in all directions (Nakamura 1989; Huan 1997), RB ≈ 1.

$$STT = RS = SHs/SVS \qquad (4)$$

This means that the transfer function (H/V spectral ratio) of the surface layer as defined by this equation may be estimated from the tremor on the surface only.

Microtremor data acquisition

Microtremor data has been collected for 76 sites as shown in Fig. 8. The Vs_{30} of these were calculated by Aldahri et al. (2017). The data acquisition was conducted using Trillium Compact 120 s and Trillium 120 PA seismometers. These seismometers are manufactured by Nanometrics Company, and they are sufficient to acquire seismic data over a wide frequency range. The used seismometers are suitable for both portable and fixed operation conditions. These seismometers have a very low self-noise. The seismic data were digitized and stored using Taurus portable seismographs. Taurus is equipped with three 24-bit data channels. Time-series data are stored in Steim (1) format, and can be extracted into MiniSEED, Seisan, or ASCII format, and streamed in Nanometrics NP format. Taurus can be deployed to record continuous data for extended periods of time. Taurus can record and store the seismic data at different sampling rates; in the current study, Taurus was adjusted to record and store the seismic data at 100 samples per second. The data acquisition was done through the summer of 2013. As the temperature and density of traffic in Jeddah during the summer are high, data acquisition was performed during the night hours in order to overcome the effect of temperature and traffic on the records. During data acquisition, all the precautions mentioned by Duval et al. (1994), Nakamura (1996), Mucciarelli et al. (1997)), Mucciarelli (1998), Mohamed (2003), and SESAME (2004) were considered. The length of the record started from 90 min to more than 3 h in case of bad recording conditions. The recorded data was tested daily. Any error within the data was discovered, and the acquisition of that site was repeated (Fig. 9).

Data processing

The H/V computations are carried out using Geopsy software which was designed under the SESAME European research project WP12 (2004). Short-duration instabilities of the signal are avoided during H/V processing through anti-trigger window selection to remove the transients. The used time window length is 40 s. These windows were automatically selected considering the short-term average (STA)/long-term average (LTA) between 0.2 and 2.5. The current analysis was carried out for the frequency range between 0.5 and 15 Hz.

The baseline effect for each microtremor record has been corrected using the running average technique. This is completed by sliding an average window of a given length over the data series. For each window, the baseline is calculated as the average value in the data window. Various numbers of windows with 40-s (4000 samples) duration were selected automatically. This time window is proven to be sufficiently long to provide stable results. The time series was tapered with a cosine taper, and an amplitude spectrum is computed for each

a

b

c

d

e
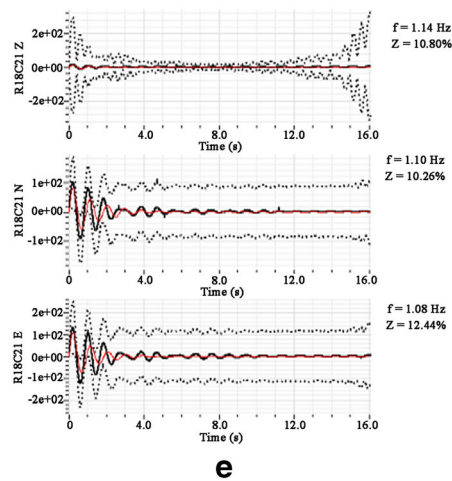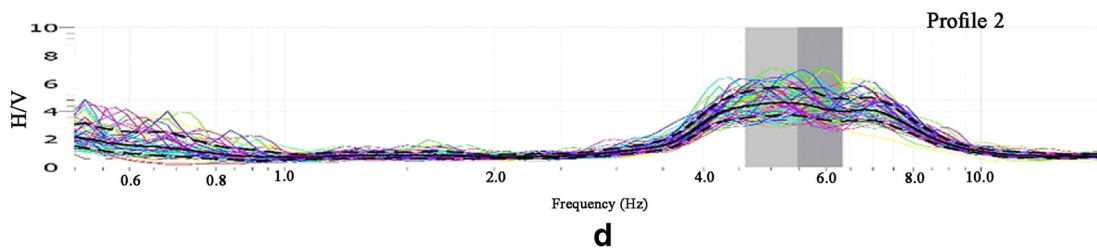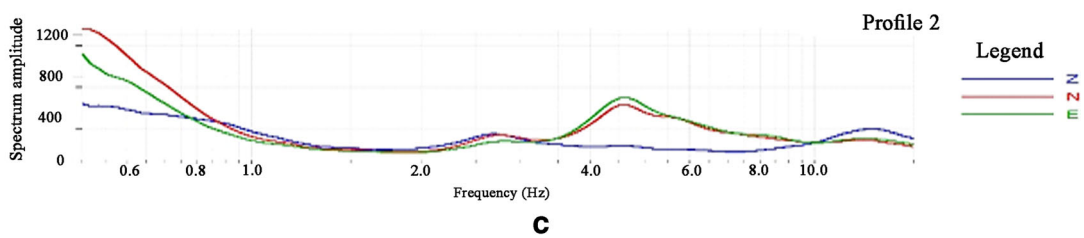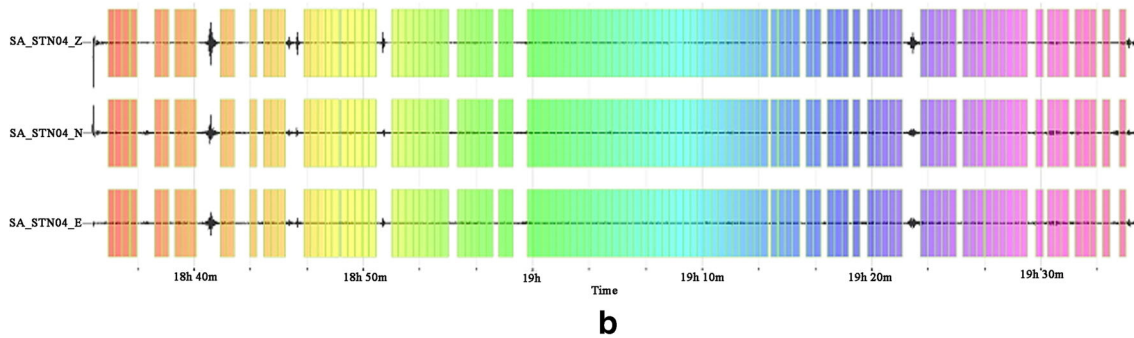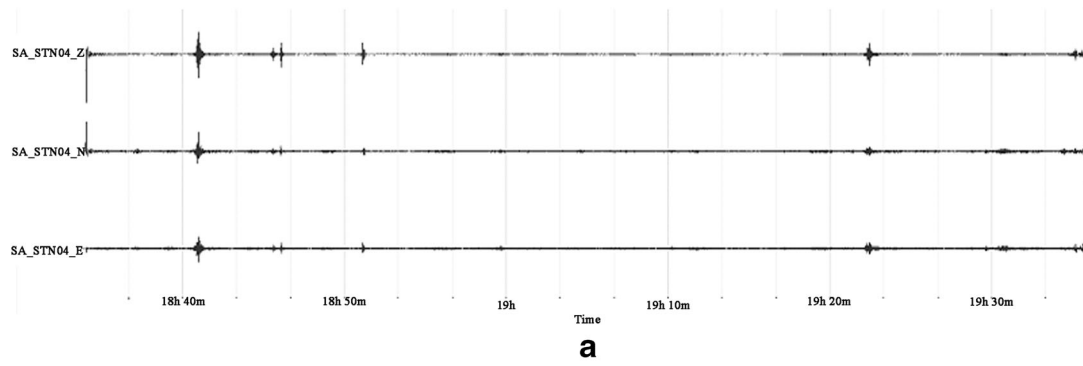
◀ **Fig. 10** Sequence of the H/V spectral ratio calculations and testing for the origin of the peak which appeared on the curve of site P2. **a** Microtremor record. **b** Window selection model. **c** Spectral curve. **d** H/V ratio curve. **e** Damping test of a peak of natural origin at 5.4 Hz

component. The FFT spectra were smoothed using the methodology of Konno and Ohmachi (1998), paying attention not to destroy the important spectral peaks. The two horizontal components were merged using the squared average methodology. H/V for each time window is calculated, then an average H/V curve is calculated. The reliability of the obtained H/V curves and peaks was examined using the criteria of the SESAME project (2004).

Microtremor records acquired in urban areas usually suffer from machinery noise. This machinery noise usually appears on the H/V curve as local narrow peaks. Discrimination between the peaks of the machinery origin and the peaks from the natural origin is very important. The origin of the obtained H/V peaks was tested using the damping test. Figure 10 shows

the sequence of data processing implemented in the current study.

Results

The dominant frequency in the study area ranges between 0.77 and 5.7 Hz as shown in Fig. 11. This frequency band matches the frequency of the engineering structures in the Ubhur area. The f_0 distribution map shows that the high resonance frequencies concentrate at the east and northeastern parts of the study area. These high dominant frequencies decrease in the west and southwest directions, while the A_0 distribution map shows that the area under investigation can amplify the seismic wave by a factor ranging between two to six times. The high amplification factors ($A_0 = 3.6$ to 6.0) are concentrated in two parts of the study area. The first part occupies the area around Ubhur Creek (Sharm of Ubhur), and the second part occupies the northeastern part of the study area (Fig. 12). The middle part of the study area shows low
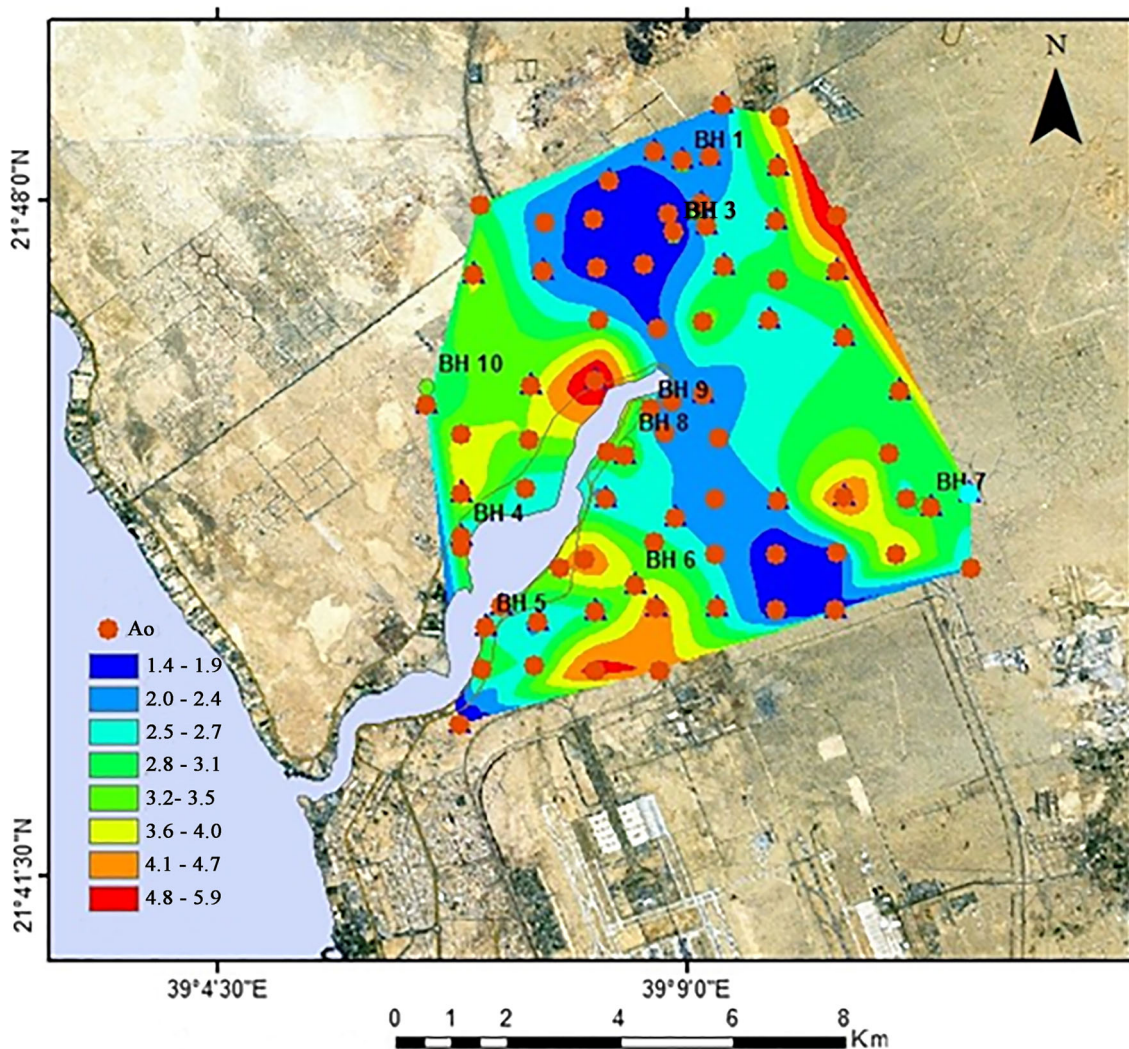
Fig. 11 Distribution of the dominant frequency (f_0) of Ubhur district
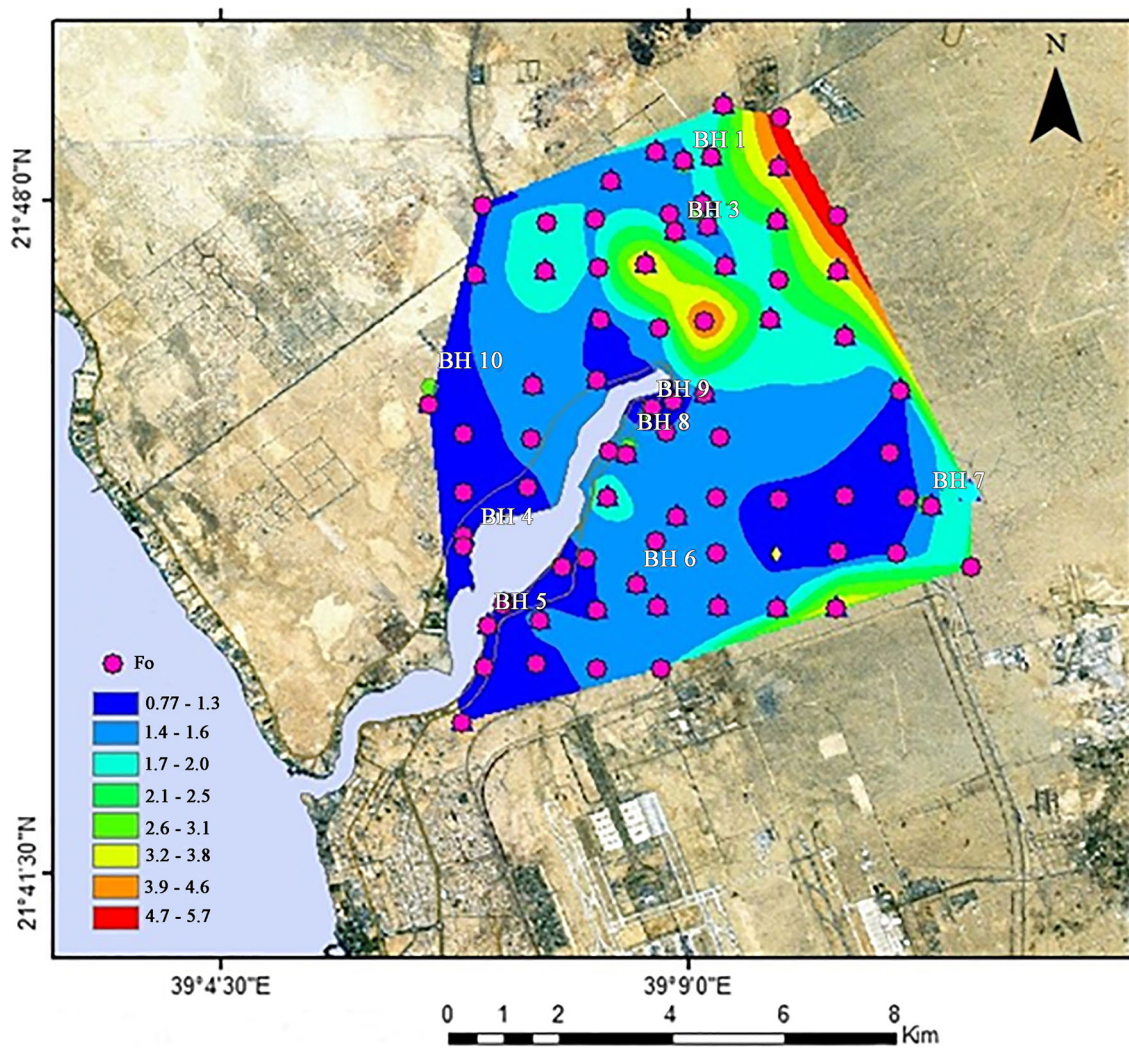
**Fig. 12** Distribution of the soil maximum amplification factor (A_0) of Ubhur district

amplification factors ($A_0 < 2.5$), while the eastern and northwestern parts of the study area are characterized by $3.5 > A_0 > 2.5$ according to the F_0 distribution map and A_0 distribution map; the study area can be classified into three zones as the following:

1. Zone (1): this zone occupies the area around Ubhur Creek and the southeastern part of the study area. This zone is characterized by f_0 ranging between 0.7 and 1.5 Hz. Concerning the distribution of A_0 in this zone, we can observe that the area south to Ubhur Greek shows high amplification factors ranging between 3.6 and 6.0 times while the area to the north of the creek shows lower amplification factors ranging between 2.5 and 3.5. Soil class C is dominant at this zone with minor occurrence of some small localities of site class B. Figure 13 shows the microtremor analysis and results of site P17 as an example of a reliable H/V curve representing the characters of this zone.

2. Zone (2): this zone occupies the middle part of the study area. This zone is characterized by f_0 ranging between 1.5 and 2.5 Hz. Concerning the distribution of A_0 in this zone, we can observe that this zone shows amplification factors less than 2.4. Soil class C is dominant at this zone. Figure 14 shows an example of a reliable H/V curve representing the characters of this zone.

3. Zone (3): this zone occupies the northeastern part of the study area. This zone is characterized by f_0 ranging between 2.5 and 5.7 Hz. Concerning the distribution of A_0 in this zone, we can observe that this zone shows amplification factors ranging between 2.5 and 3.5. Soil classes C and D are dominating this zone. Figure 15 shows an example of a reliable H/V curve representing the characters of this zone (Fig. 16).

Fig. 13 Sequence of the H/V spectral ratio calculations and testing for the ▶ origin of the peak which appeared on the curve of site P34. **a** Microtremor record. **b** Window selection model. **c** Spectral curve. **d** H/V ratio curve. **e** Damping test
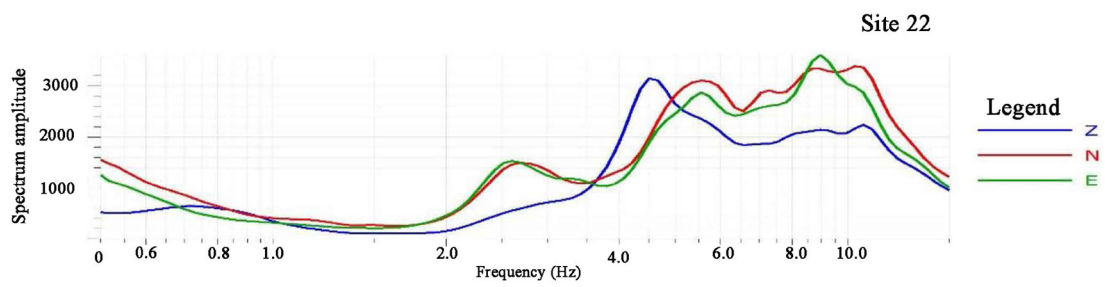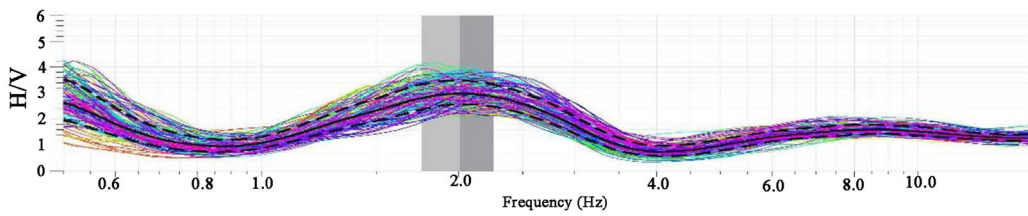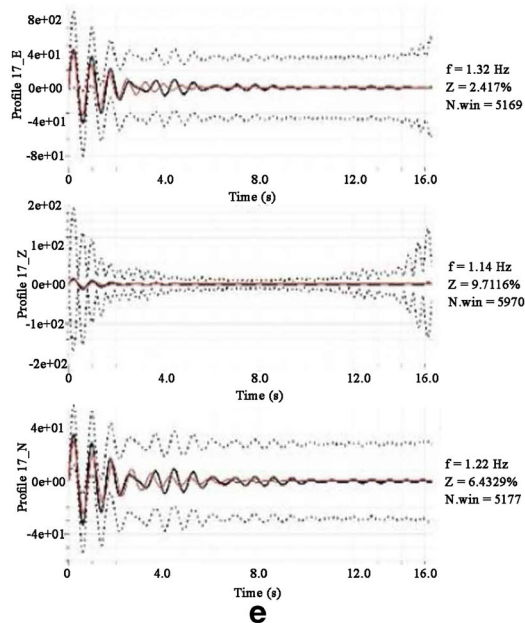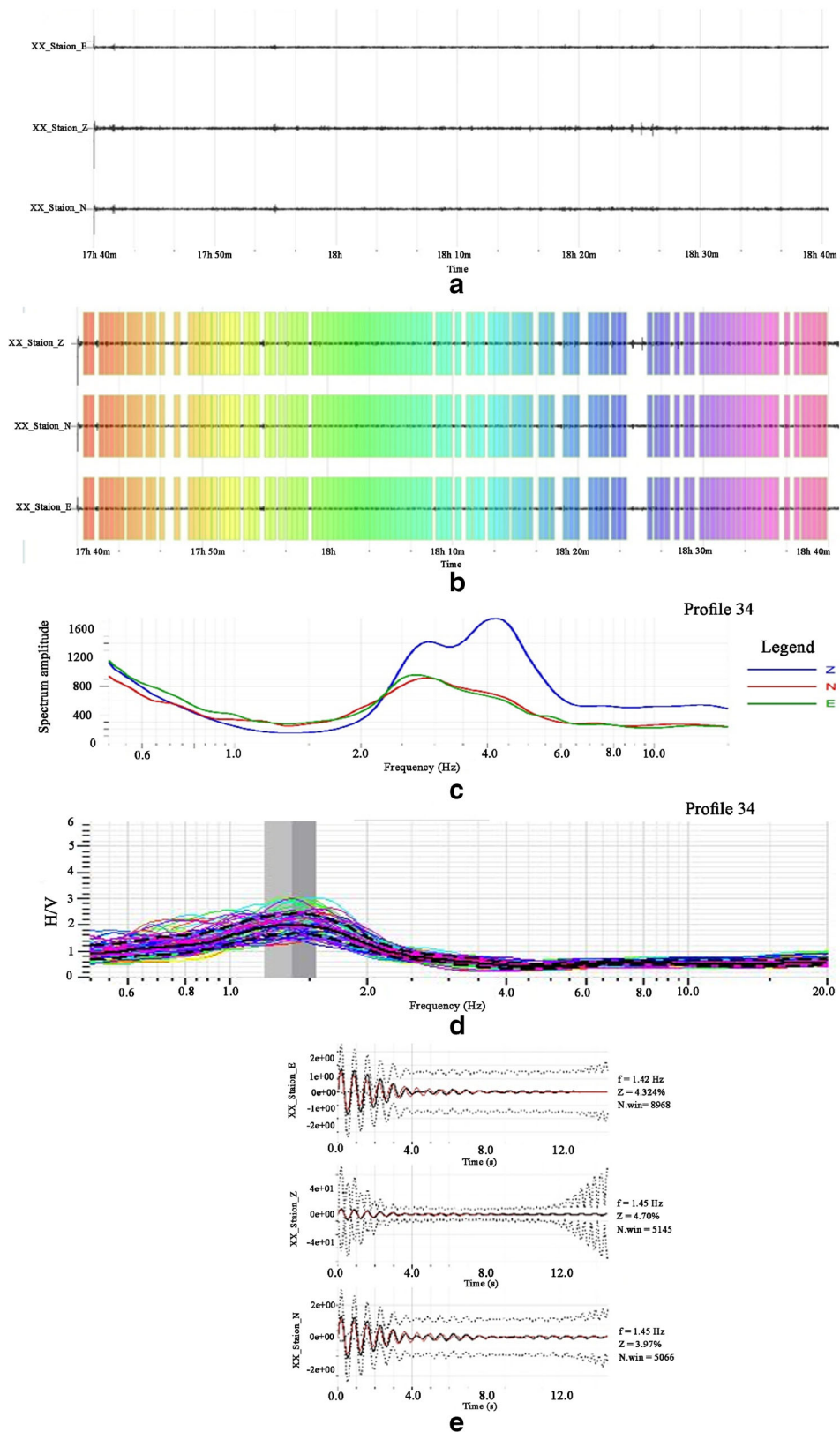
a

b

Site 22
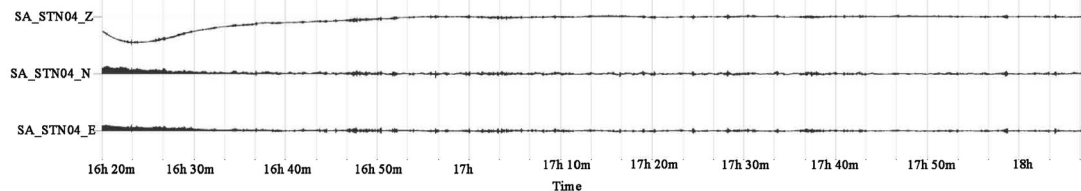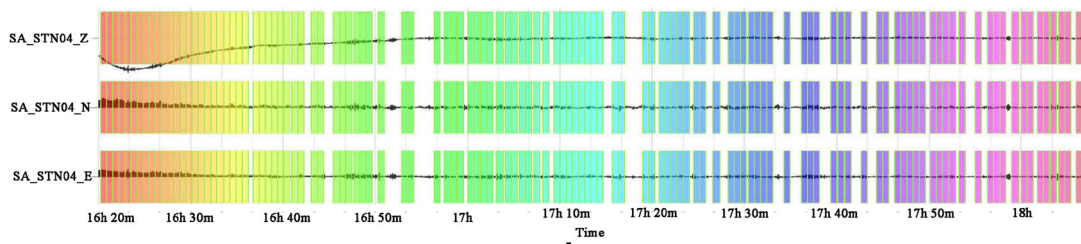
c

profile 22

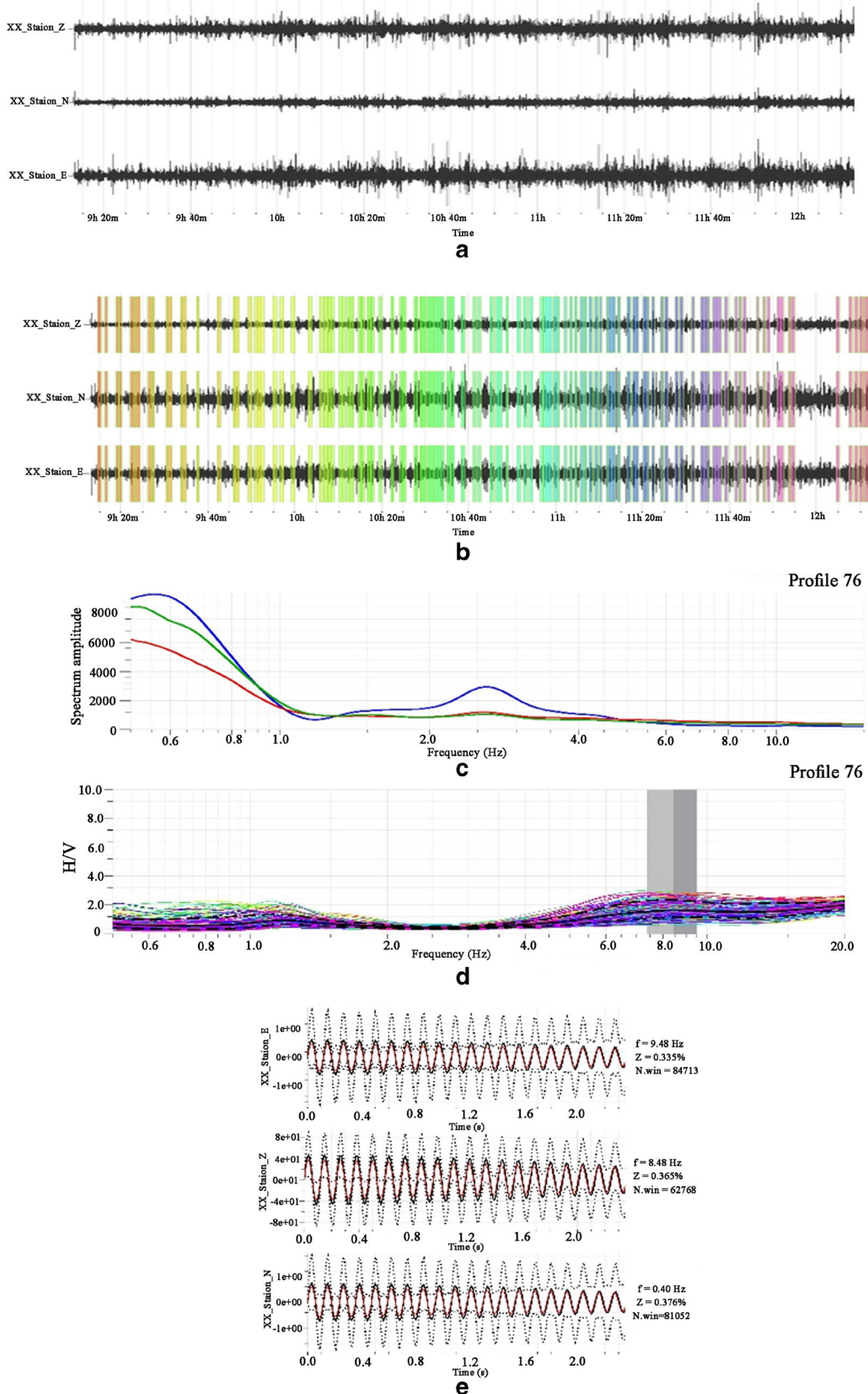
d

e

Fig. 14 Sequence of the H/V spectral ratio calculations and testing for the origin of the peak which appeared on the curve for a site in the western part of the study area P76. **a** Microtremor record. **b** Window selection model. **c** Spectral curve. **d** H/V ratio curve. **e** Damping test

Fig. 15 Sequence of the H/V spectral ratio calculations and testing for the origin of the peak appeared on the curve of the site P34. **a** Microtremor record. **b** Window selection model. **c** Spectral curve. **d** H/V ratio curve. **e** Damping
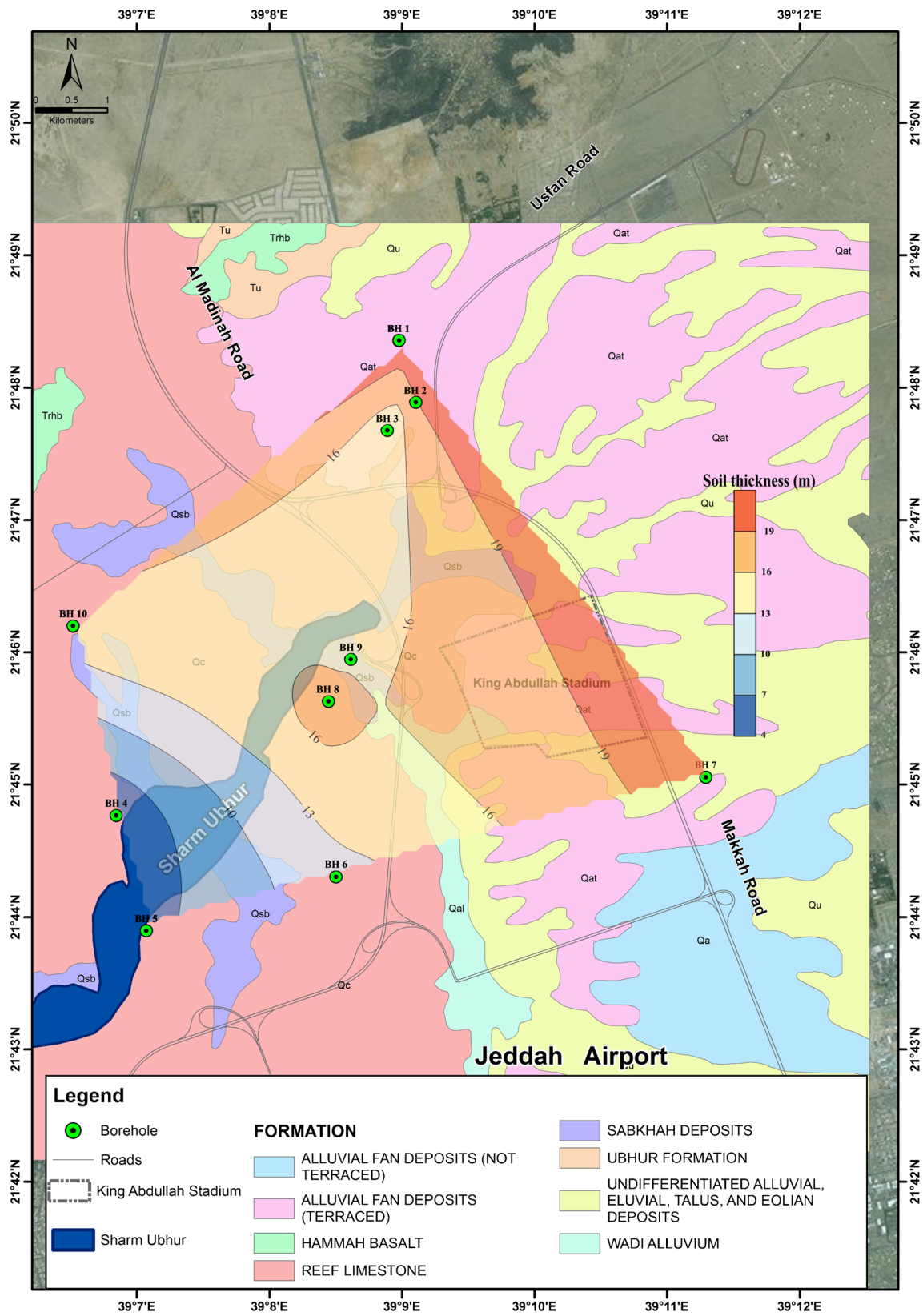
Fig. 16 Soil thickness map of the study area (Aldahri et al. 2017)

Discussion and conclusions

Al-Qarni (2015) studied the microzonation of the Jeddah urban area which is located at the south of our study area using both microtremor data and the multianalysis of surface waves. The author found that the resonance frequency ranges between 0.48 and 4.87 Hz and the maximum amplification factor ranges between 1 and 7. The resonance frequency range and maximum amplification of Jeddah coincide with the resonance frequency range and maximum amplification factor of Ubhur. We suggest that the soils of two regions have the same subsurface soil conditions and structures. Also, the f_0 maps of the current have the same pattern as the maps produced by Al-Qarni (2015), where the low f_0 values are concentrated on the west part (near the Red Sea Coast), and these values are increasing gradually to the east.

The A_0 map showed a range of small values extending north-south, indicating the presence of the foundation layer near the Earth's surface, while these values increased eastward and westward, indicating the presence of large thickness of soft sediments in the eastern part of the Ubhur area. In addition, BH 1 is located within the range between 2.4 and 2 of the amplification factor (these values are considered small) while it lies in the range from 2.1 to 2.5, with f_0 considered to be relatively high from the engineering point of view. In addition, the southeastern part in the A_0 map has the lowest values of the frequencies. This indicates that the foundation layer is deep while the surface soil is composed of soft deposits. In comparison with the geological map of Ubhur, the southeastern zone is composed of sabkha deposits. It is indicated that the central zone of the Ubhur district is considered suitable for the construction of high-rise facilities compared to other parts of the region, which should be taken into consideration during land use planning.

References

Aldahri M, Mogren S, Abdelrahman K, Zahran H, El Hady S, El-Hadidy M (2017) Surface soil assessment in the Ubhur area, north of Jeddah, western Saudi Arabia, using a multichannel analysis of surface waves method. J Geol Soc India 89(4):435–443. https://doi.org/10.1007/s12594-017-0626-7

Ali KM, Hossain D (1988) Geotechnical and geochemical characteristics of Ubhur sub-soil. J.K.A.U. Earth Sci 1:205–225

Al-Qarni H (2015) Seismic microzonation of Jeddah City, Western Saudi Arabia, Msc thesis, Geophysics Department (Geophysics), Faculty of Science, King Saud University

Al-Saifi MM, Qari MY (1996) Application of Landsat thematic mapper data in sabkha studies at the Red Sea coast. Int J Remote Sens 17(3):527–536. https://doi.org/10.1080/01431169608949025

Ambraseys NN, Melville CP, Adams RD (1994) The seismicity of Egypt, Arabia and the Red Sea: a historical review. Cambridge University Press, UK, p 181. https://doi.org/10.1017/CBO9780511524912

Aqeel AM (2007) Geotechnical investigation of sabkha hazards at the northern part of Obhor area. Thesis of Degree Master of Science in Applied Geology (Engineering Geology). Faculty of Earth Sciences (King Abdulaziz University)

Bahafzullah A, Fayed LA, Kazi A, Al-Saify M (1993) Classification and distribution of the Red Sea coastal sabkha near Jeddah-Saudi Arabia. Carbonate Evaporates 8(1):23–38. https://doi.org/10.1007/BF03175160

Bosworth W, Huchon P, McClay K (2005) The Red Sea and the Gulf of Aden basins. J Afr Earth Sci 43(1-3):334–378. https://doi.org/10.1016/j.jafrearsci.2005.07.020

Duval AM, Bard PY, Meneroud JP, Vidal S (1994) Usefulness of microtremor measurements for site effect studies. In: Duma G (ed) Proceedings of the tenth European conference on earthquake engineering, Vienna, Austria, I. Balkema, Rotterdam, pp 521–528

El-Hadidy SY (2015) Seismicity and seismotectonic setting of the Red Sea and adjacent areas. In: Rasul NMA, Stewart ICF (eds) The Red Sea. Springer Earth System Sciences, Berlin, pp 151–159. https://doi.org/10.1007/978-3-662-45201-1_8

Huan C (1997) The validity of single-station H/V ratio for site response estimation using the dahan downhole array, Hualien, Taiwan, TAO, The Ministry of Economic Affairs, Taiwan

Johnson PR (1999) Proterozoic geology of western Saudi Arabia–Southern sheet: Saudi Geological Survey Open-File Report USGS-OF-99-7

Konno K, Ohmachi T (1998) Ground motion characteristics estimated from spectral ratio between horizontal and vertical components of microtremor. Bull Seismol Soc Am 88:228–241

Lermo J, Chaves-Garcia FJ (1993) Site effect evaluation using spectral ratios with only one station. Bull Seismol Soc Am 83(5):1574–1594

Mohamed A (2003) Estimating earthquake ground motions at the north-western part of the Gulf of Suez, Egypt. Ph.D. thesis, Fac. Sc., Ain Shams Uni. Pp 93–138

Morris PG (1975) Construction materials, non-metallic minerals occurrence and engineering geology of the district around Jeddah, Dir. Gen. Miner. Resour., Technical Record TR-75-1, 27P. Kingdom of Saudi Arabia

Mucciarelli M (1998) Reliability and applicability of Nakamura's technique using microtremors: an experimental approach. J Earthq Eng 2(4):1–14

Mucciarelli M, Contri P, Monachesi G, Calvano G (1997) Towards an empirical method to instrumentally assess the seismic vulnerability of existing buildings, Proceedings of Conference on Disaster Mitigation and Information Technology, London

Nakamura Y (1989) A method for dynamic characteristics estimation of subsurface using microtremor of the ground surface QR of RTRI. 30(1):89–94

Nakamura Y (1996) Real-time information systems for hazards mitigation. Proceedings of the 11th World Conference on Earthquake Engineering, Acapulco, Mexico

Roobol MJ, Al-Rehaili M, Arab N, Celebi M, Halawani MA, Janjou D, Kazi A, Martin C, Sahl M, Showail A (1999) The Gulf of Aqaba earthquake of 22 November 1995: its effects in Saudi Arabia. Saudi Arabian Deputy Ministry for Mineral Resources Technical Report BRGM-TR-99-16, 67 p 49 figs, 4 tables, 1 appendix

SESAME (2004) Site effects assessment using ambient excitations, European research Project. http://sesamefp5.obs.ujf-grenoble.fr

Zahran HM, Sokolov VM, Roobol J, Stewart IC, El-Hadidy SY, El-Hadidy M (2016) On the development of a seismic source zonation model for seismic hazard assessment in western Saudi Arabia. J Seismol 20(3):747–769. https://doi.org/10.1007/s10950-016-9555-y